

Electronic Supplementary Information (ESI)  
for  
ChemComm

# A red fluorescent turn-on probe for hydrogen sulfide and its application in living cells

Xingyu Qu,<sup>a</sup> Cuijuan Li,<sup>a</sup> Huachao Chen,<sup>a</sup> John Mack,<sup>b</sup> Zijian Guo\*<sup>a</sup> and Zhen Shen\*<sup>a</sup>

<sup>a</sup> State Key Laboratory of Coordination Chemistry, Nanjing University, Nanjing, 210093, PR China.  
[zshen@nju.edu.cn](mailto:zshen@nju.edu.cn),

<sup>b</sup> Department of Chemistry, Rhodes University, Grahamstown 6140, South Africa

## Table of Contents

I.	Experimental details
I.1	Materials and methods
I.2	Quantum yields determination
I.3	Cell culture and fluorescence bioimaging
I.4	Synthesis section
I.5	Theoretical calculations
II.	Supplementary data
II.1	Figure S1. <sup>1</sup> H NMR spectrum of <b>3</b> .
II.2	Figure S2. <sup>1</sup> H NMR spectrum of <b>1</b> .
II.3	Figure S3. H-H COSY spectrum of <b>1</b> .
II.4	Figure S4. <sup>13</sup> C NMR spectrum of <b>1</b> .
II.5	Figure S5. HR-MS spectrum of <b>1</b> .
II.6	Figure S6. MALDI-TOF MS spectrum of <b>Cu-1</b> .
II.7	Figure S7. Job's plot for determining the stoichiometry of the reaction between <b>1</b> and Cu <sup>2+</sup> .
II.8	Figure S8. Changes in the fluorescence spectrum of <b>1</b> as the Zn <sup>2+</sup> concentration is increased.
II.9	Figure S9. The fluorescence spectrum of <b>Cu-1</b> upon addition of various anion ions.
II.10	Figure S10. Time course of the reaction of <b>Cu-1</b> with NaHS.
II.11	Figure S11. The frontier $\pi$ -MOs of <b>1</b> in B3LYP geometry optimizations.
II.12	Figure S12. The TD-DFT calculations of the UV-visible absorption spectra of <b>1</b> and <b>Cu-1</b>
II.13	Figure S13. The UV-visible absorption spectra of <b>1</b> and <b>Cu-1</b>
II.14	Figure S14. Normalized fluorescence intensity profile for <b>1</b> .
II.15	Figure S15. Three-dimensional fluorescence images of live Hela cells for <b>1</b> .
II.16	Figure S16. MTT assay of <b>1</b> and <b>Cu-1</b> .

## I. Experimental details

### I.1 Materials and methods

Unless otherwise noted, all reagents or solvents were obtained from commercial suppliers and used without further purification. All air and moisture sensitive reactions were carried out under an argon atmosphere. Dry  $\text{CH}_2\text{Cl}_2$  was obtained by refluxing and distilling over  $\text{CaH}_2$  under nitrogen. Dry THF was distilled from sodium / benzophenone. The  $^1\text{H}$  and  $^{13}\text{C}$  NMR spectroscopic measurements were made by using a Bruker 500 MHz spectrometer. The measurements for  $^1\text{H}$  and  $^{13}\text{C}$  NMR were performed at 500 (DRX-500), and 125 MHz (DRX-500), respectively. Mass spectra were measured with a Bruker Daltonics Autoflex II<sup>TM</sup> MALDI-TOF MS spectrometer. Fluorescence spectral measurements were carried out by using an Hitachi F-4600 fluorescence spectrophotometer. Electronic absorption spectra were recorded with a Shimadzu UV-2550 spectrophotometer.

### I.2 Quantum Yields determination

Spectra were measured in 1 cm quartz cuvettes with spectroscopic grade solvents. The slit width was set at 5 nm for both excitation and emission measurements.<sup>S1</sup> Cresyl violet perchlorate in methanol ( $\phi_f = 0.55$ ) was used as the standard for the fluorescent quantum yield calculation using the absorption of the test sample. The emission spectra area was obtained from 550-800 nm. Dilute solutions ( $10^{-6}$  M) were used to minimize reabsorption effects. Fluorescence measurement were made three times for each dye and averaged. Quantum yields were determined using the following equation:

$$\Phi_{\text{samp}} = (\Phi_{\text{stand}} \times F_{\text{samp}}/F_{\text{stand}}) \times (A_{\text{samp}}/A_{\text{stand}}) \times (n_{\text{samp}}^2/n_{\text{stand}}^2)$$

$\Phi_{\text{samp}}$  is the quantum yield of the cresyl violet perchlorate standard.  $F_{\text{samp}}$  and  $F_{\text{stand}}$  are the areas under the emission spectra of the sample and standard.  $A_{\text{samp}}$  and  $A_{\text{stand}}$  are the absorbance values for the sample and standard at the excitation wavelength.  $n_{\text{samp}}$  and  $n_{\text{stand}}$  are the refractive index values of the solvents used for the sample and standard measurements. Molar extinction coefficients were obtained from the slope of a graph of absorbance vs concentration for each dye at five different concentrations ( $10^{-6}$  M).

### I.3 Cell culture and fluorescence bioimaging

The HeLa cell line was provided by the Institute of Biochemistry and Cell Biology, SIBS, CAS (China). Cells were grown in high glucose Dulbecco's Modified Eagle Medium (DMEM, 4.5 g of glucose/L) supplemented with 10% fetal bovine serum (FBS) at 37 °C and 5%  $\text{CO}_2$ . Cells ( $5 \times 10^8/\text{L}$ ) were plated on 14 mm glass coverslips and allowed to adhere for 24 h. Experiments to assess  $\text{Cu}^{2+}$  uptake were performed over 1 h in the same medium supplemented with 50  $\mu\text{M}$   $\text{Cu}(\text{CH}_3\text{COO})_2$ , and to assess  $\text{HS}^-$  uptake were performed over 1 h in the same medium supplemented with 50  $\mu\text{M}$  NaHS.

Immediately before the experiments, cells were washed with PBS buffer and then incubated with 10  $\mu\text{M}$  **1** in PBS buffer (predissolved in DMSO solution) for 30 min at 37 °C. Cell imaging was then carried out after washing the cells with PBS buffer. Confocal fluorescence imaging was performed with a Zeiss LSM 710 laser scanning microscope and a 63 $\times$ oil-immersion objective lens. Cells incubated with **1** were excited at 543 nm using a multi-line argon laser.

### I.4 Theoretical calculations

Geometry optimization and TD-DFT calculations were carried out for dipyrromethene, **1**, **Cu-1** using the B3LYP functional of the Gaussian09 software packages<sup>S2</sup> with 6-31G(d) basis sets on the sun cluster at the Centre for High Performance Computing in Cape Town, South Africa.

#### I.4 Synthesis section

Ethylphenanthro[9,10-*c*]-pyrrole-1-carboxylate **3** was synthesized according to the published procedures.<sup>S3</sup> White solid; 61% yield. <sup>1</sup>H NMR(CDCl<sub>3</sub>, 500 MHz): 9.98 (s, 1H), 9.82 (d, 1H, *J* = 10 Hz), 8.58 (d, 1H, *J* = 10 Hz), 8.54 (d, 1H, *J* = 10 Hz), 8.09 (d, 1H, *J* = 10 Hz), 7.80 (d, 1H, *J* = 5 Hz), 7.61 (m, 2H), 7.52 (m, 2H), 4.49 (q, 2H, *J* = 10 Hz), 1.48 (t, 3H, *J* = 3.0 Hz).

##### Compound 1

The 1-methylphenanthro[9,10-*c*]pyrrole **2** was synthesized according to the published procedures. <sup>S3</sup> **2** (480 mg, 5.02 mmol) and triethyl orthoformate (600 mg, 2.52 mmol) were dissolved in dry CH<sub>2</sub>Cl<sub>2</sub> (100 mL) under an argon atmosphere. One drop of trifluoroacetic acid (TFA) was added, and the solution was stirred for 48 h at ambient temperature in the dark (until TLC indicated complete consumption of the aldehyde). The dark brown reaction mixture was washed twice with 50 mL water and 50 mL brine, dried over Na<sub>2</sub>SO<sub>4</sub>, and concentrated at reduced pressure. The crude product was purified by silica-gel column chromatography (dichloromethane), and then by neutral alumina column chromatography (dichloromethane-petroleum: ether, 1:1, v/v).

**1**: black solid; 26% yield; m.p. > 250 °C; <sup>1</sup>H NMR(THF-*d*<sub>8</sub>, 500 MHz): 8.80 (s, 1H), 8.78 (d, 4H, *J* = 5 Hz), 8.74 (d, 2H, *J* = 10 Hz), 8.44 (d, 2H, *J* = 5 Hz), 7.77 (t, 2H, *J* = 10 Hz), 7.63 (q, 4H, *J* = 10 Hz), 7.54 (t, 2H, *J* = 10 Hz), 3.09 (s, 6H); <sup>13</sup>C NMR(THF-*d*<sub>8</sub>, 125 MHz): 127.2, 126.9, 126.2, 125.0, 124.4, 124.0, 123.5, 123.4, 18.54. HR-MS, Calcd. for (C<sub>32</sub>H<sub>31</sub>BF<sub>2</sub>N<sub>7</sub>): 472.1939; Found: 472.1934 [*M*<sup>+</sup>].

##### Compound Cu-1

**1** (0.1 mmol, 50 mg) and copper(II) acetate (0.5 mmol, 200 mg) were added to a 100 mL round bottomed flask containing 100 mL tetrahydrofuran, and the solution was stirred for 24 h at ambient temperature in the dark. When all the starting material had dissolved, the mixture was concentrated at reduced pressure. The products were the remainder that the mixture was washed with 100 mL of water.

Compound **Cu-1**: black solid; 100% yield; m.p. > 250 °C; MALDI-TOF MS, Calcd: 1005; Found: *m/z*: 1005(*M*<sup>+</sup>).

## II Supplementary data

### II.1

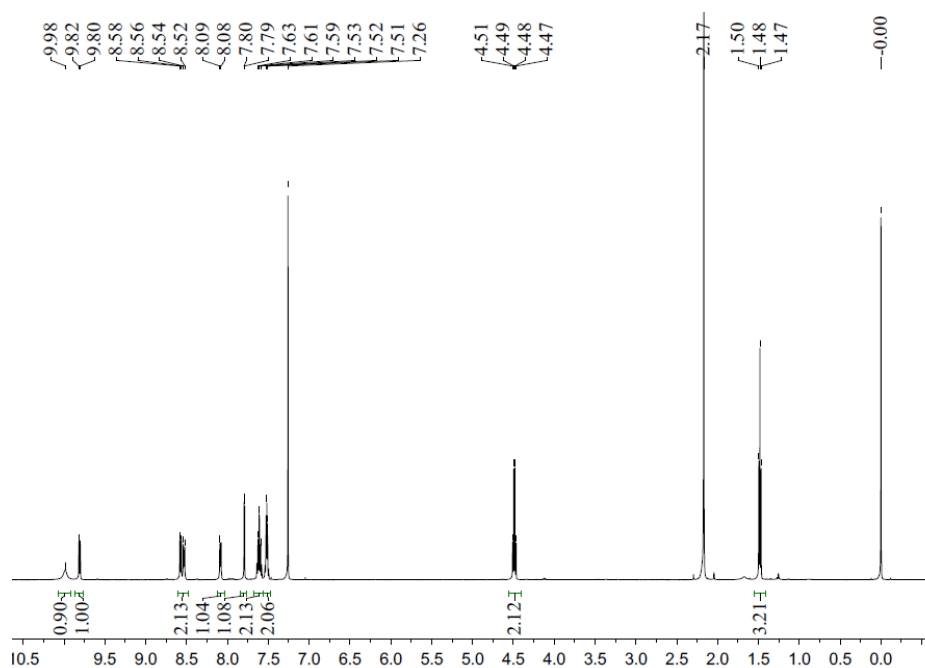


**Figure S1.**  $^1\text{H}$  NMR spectrum of **3**.

II.2

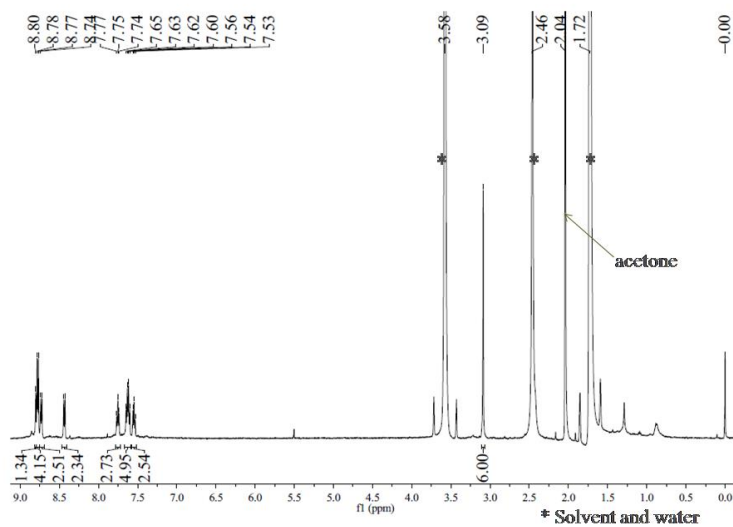


**Figure S2.** <sup>1</sup>H NMR spectrum of **1**.

II.3

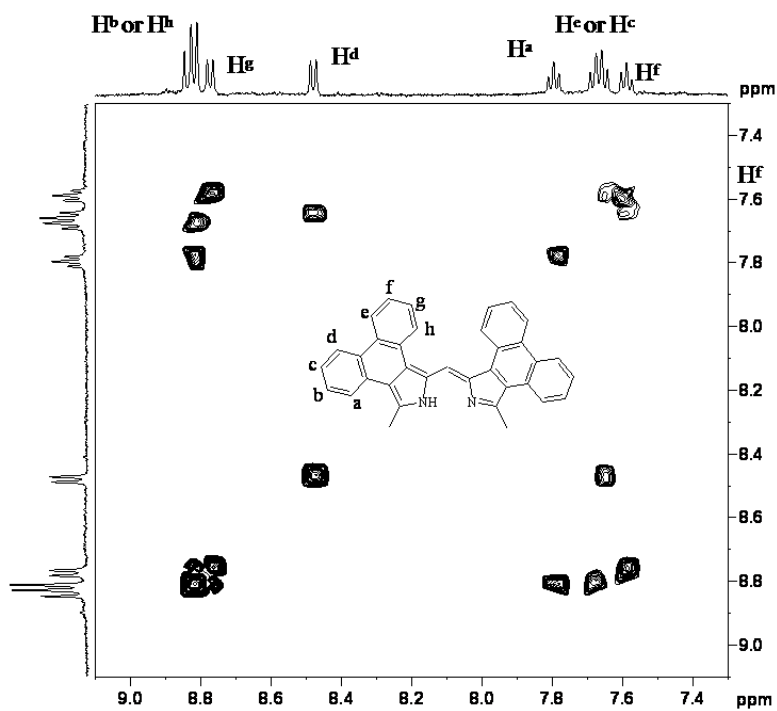
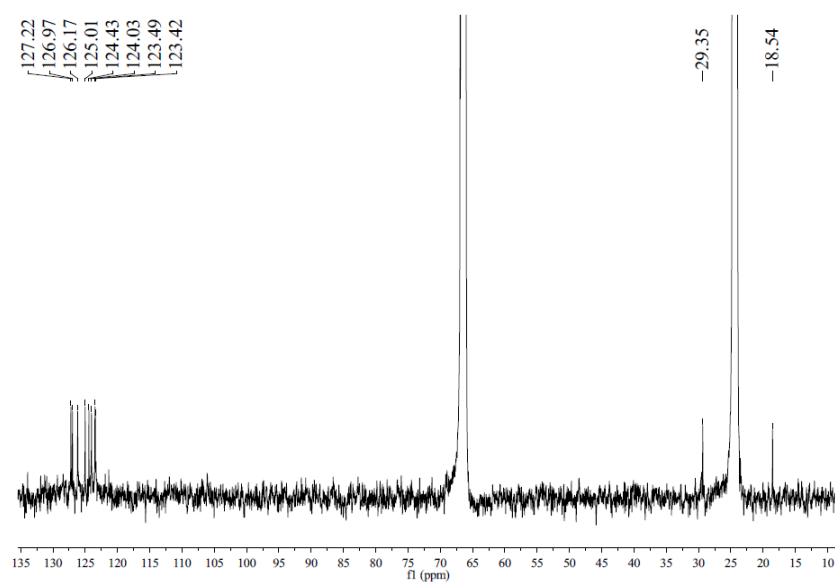


Figure S3.  $^1\text{H}$ -H COSY spectrum of **1**.

II.4



**Figure S4.** <sup>13</sup>C NMR spectrum of **1**.

II.5

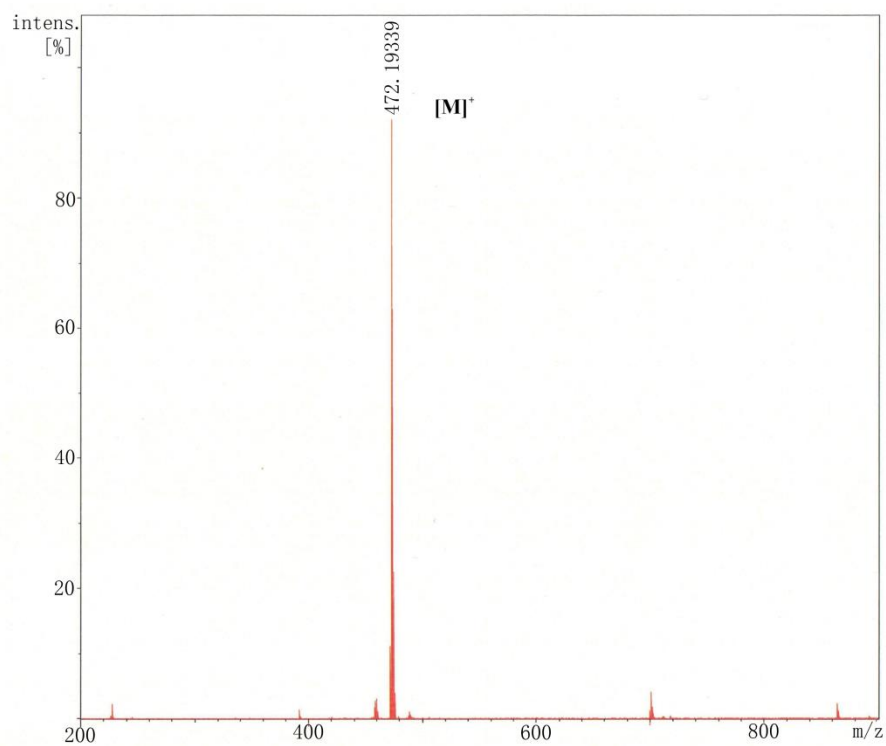


**Figure S5.** HR-MS spectrum of **1**.



II.6

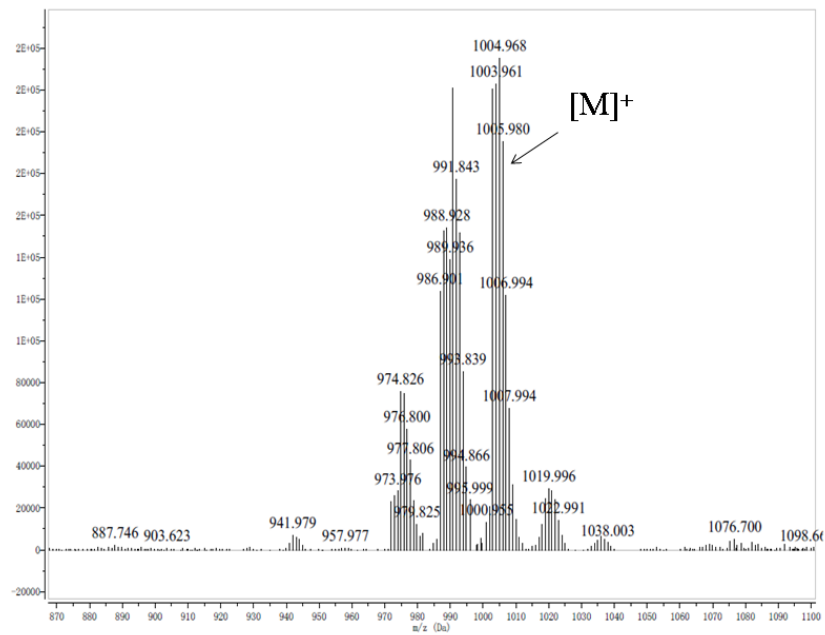


**Figure S6.** MALDI-TOF MS spectrum of **Cu-1**.

II.7

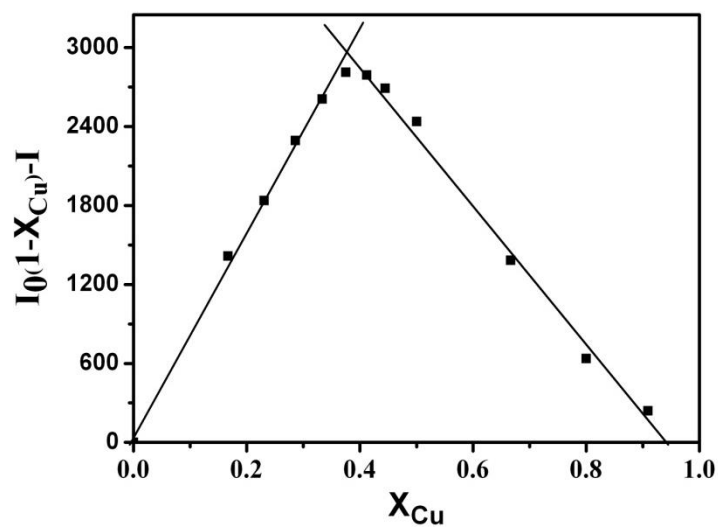


**Figure S7.** Job plot for determining the stoichiometry of the reaction between **1** and  $Cu^{2+}$  (20  $\mu M$  in DMSO/ $H_2O$ , 4:1, v/v,  $\chi_{Cu} = [Cu^{2+}]/([Cu^{2+}] + [1])$ ) at an excitation wavelength of 540 nm.

II.8

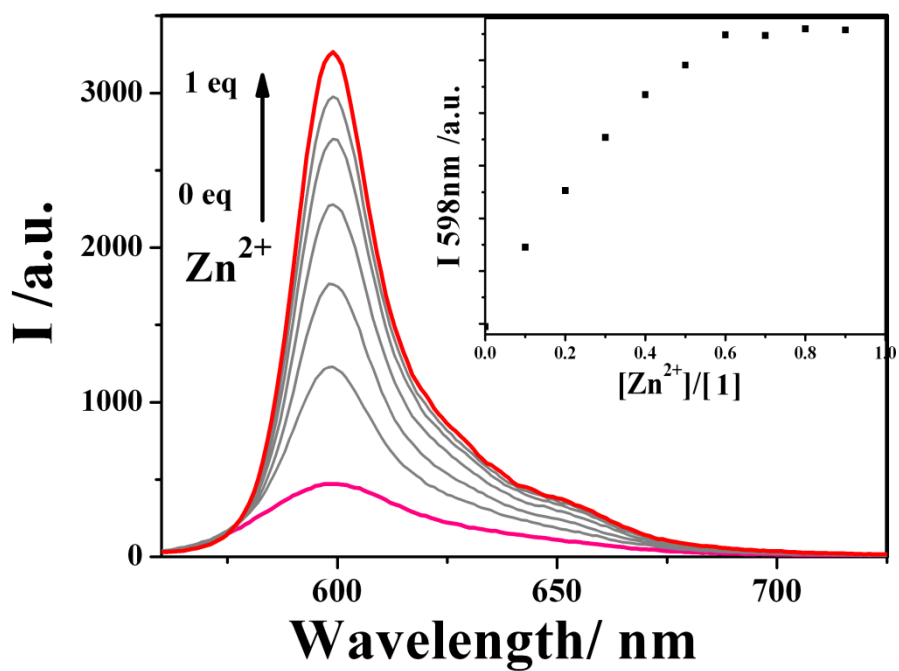


**Figure S8.** Changes in the fluorescence spectrum of **1** (20  $\mu\text{M}$  in DMSO/  $\text{H}_2\text{O}$ , 4/1) as the  $\text{Zn}^{2+}$  concentration is increased.

II.9

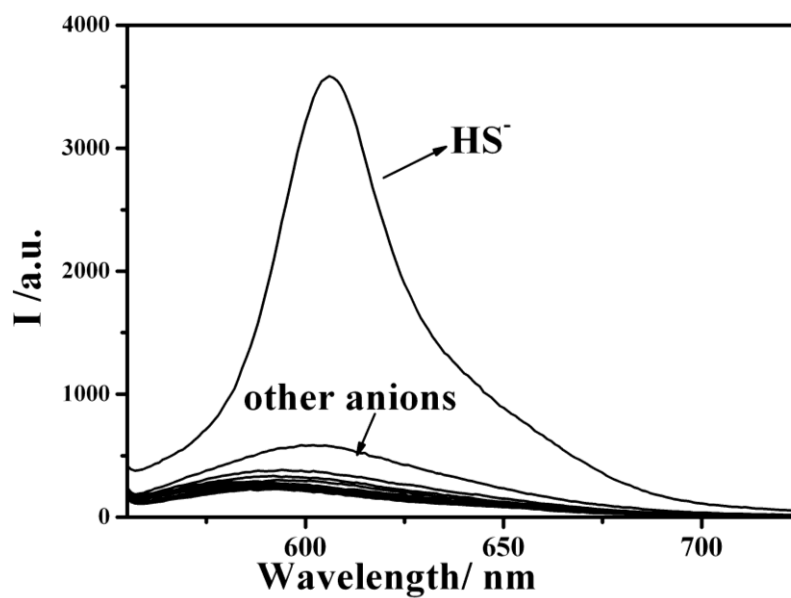


**Figure S9.** The fluorescence spectra of **Cu-1** recorded at upon the addition of various anion ions.

II.10

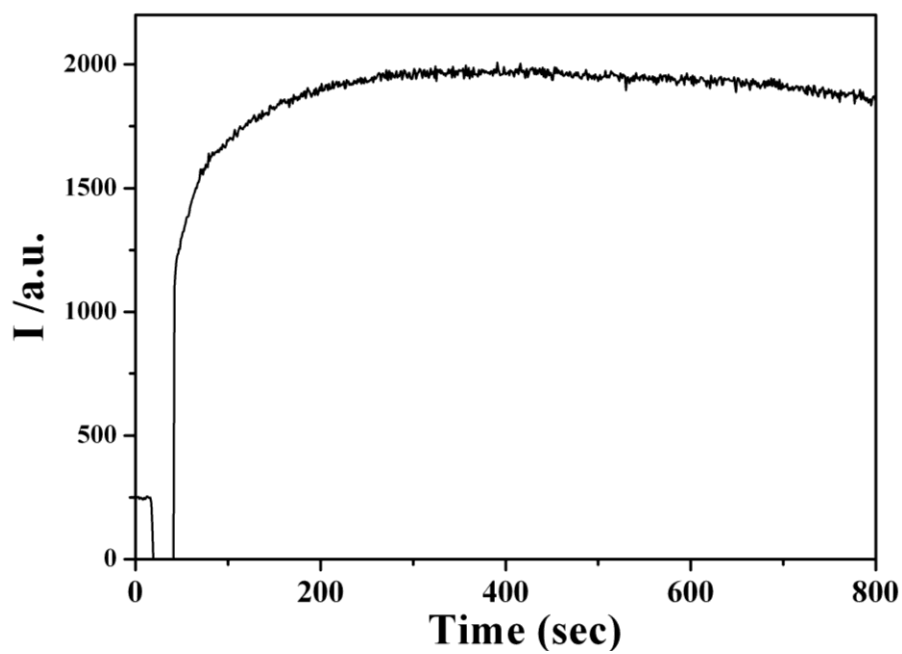


**Figure S10.** Time course of change in fluorescence intensity during the reaction between **Cu-1** and  $\text{HS}^-$  after the addition of 1.5eq NaHS in DMSO- $\text{H}_2\text{O}$  (4:1, v:v) solution with an intense band at 600 nm ( $\lambda_{\text{ex}} = 540$  nm).

II.11

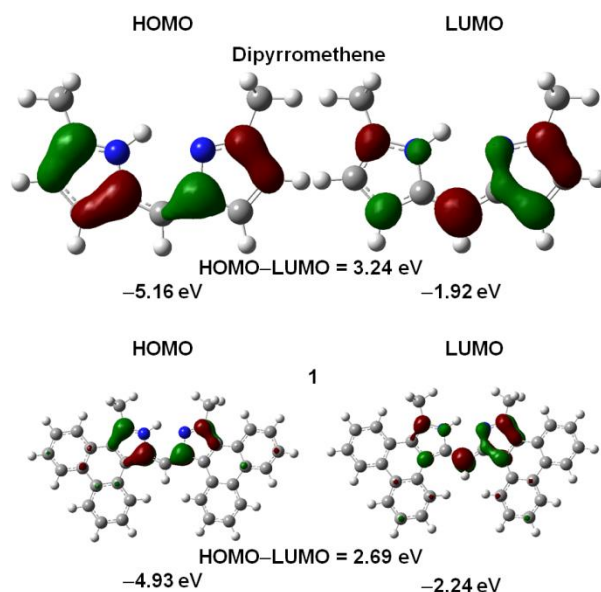


**Figure S11.** The frontier  $\pi$ -MOs of **1** and the corresponding dipyrromethene compound predicted in B3LYP geometry optimizations with 6-31G(d) basis sets carried out using the Gaussian 09 software package.<sup>S2</sup> The narrowing of the HOMO-LUMO gap due to fused-ring-expansion with phenanthrene moieties results in a marked red shift of the main BODIPY absorption and emission bands (Fig. 1)

## II.12

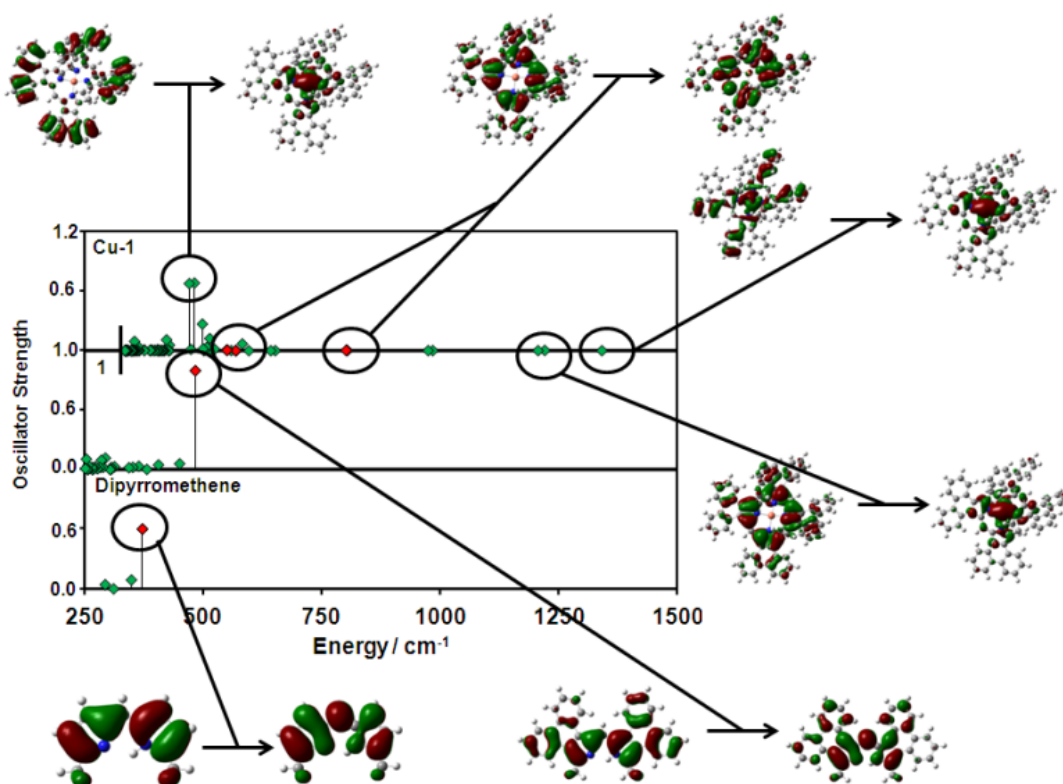


**Figure S12.** The TD-DFT calculations of the UV-visible absorption spectra of dipyrromethene, **1** and **Cu-1** predicted by using the B3LYP functional of the Gaussian 09 software package<sup>S2</sup> with 6-31G(d) basis sets. The band energies are denoted by green diamonds. Red diamonds are used to highlight the transitions associated with the MOs derived from the HOMO and LUMO of the dipyrromethene  $\square$ -system. The MOs involved with the one-electron transitions which provide the major contributions to the most significant spectral bands are shown at an isosurface value of 0.02 a.u.

II.13

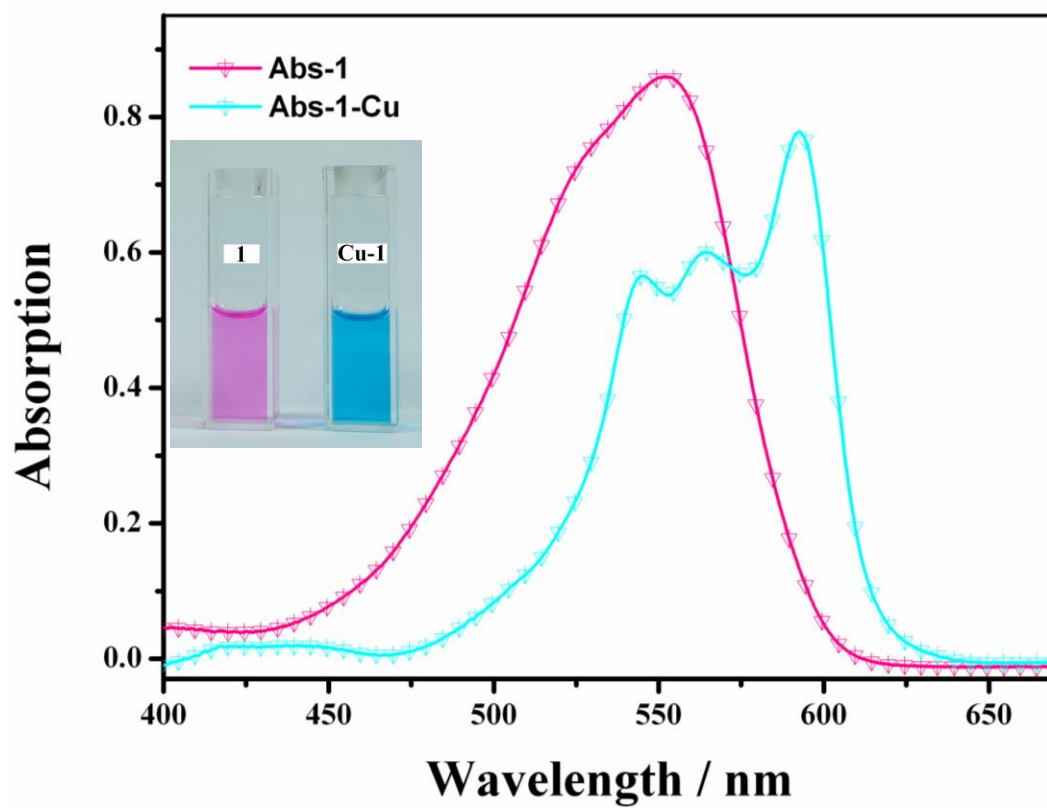


**Figure S13.** The UV-visible absorption spectra of **1** (red line) and **Cu-1** (blue line).



II.14

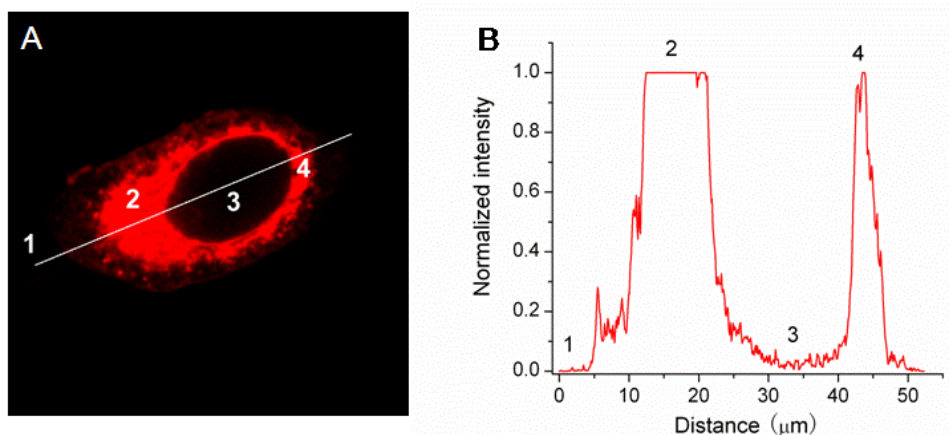


**Figure S14.** (A) Confocal fluorescence imaging of living HeLa cells incubated with 10  $\mu\text{M}$  **1** for 30 min at 25  $^{\circ}\text{C}$ . (B) Normalized fluorescence intensity profile across the line shown in panel A corresponding to cytoplasm (1), nuclear region (2 and 4), and cytoplasm (3).

II.15

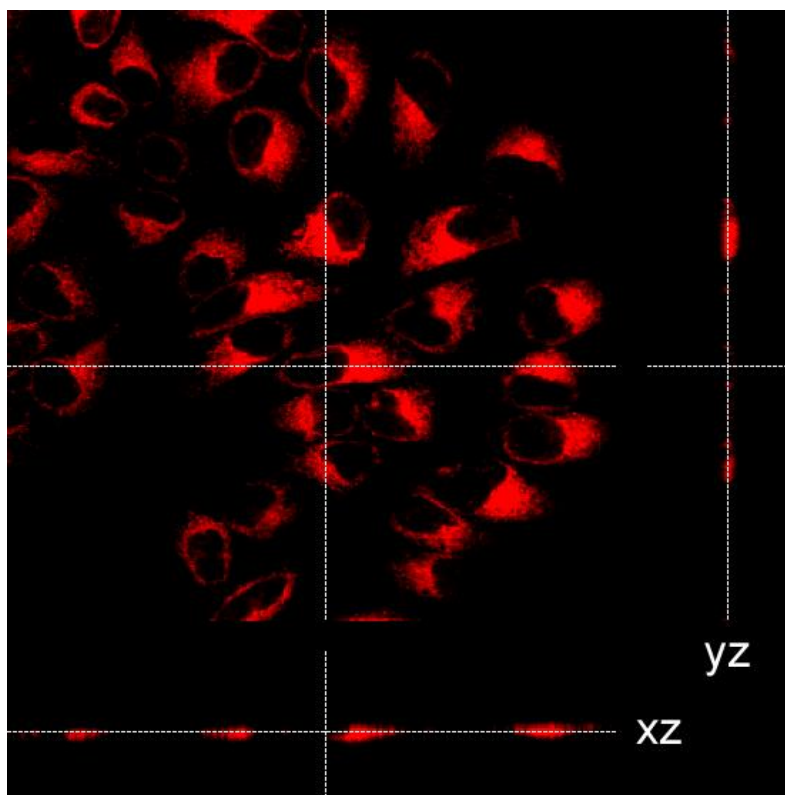


**Figure S15.** Three-dimensional fluorescence images of live HeLa cells loaded with 10  $\mu\text{M}$  **1** for 30 min at 25  $^{\circ}\text{C}$ . Panel A is an *xy*-image obtained at  $z = 2174.72 \mu\text{m}$ , while panels B and C display the *yz*- and *xz*- cross sections ( $z = 2154.52\text{--}2201.94 \mu\text{m}$ ) taken at the lines shown in panel A, respectively.

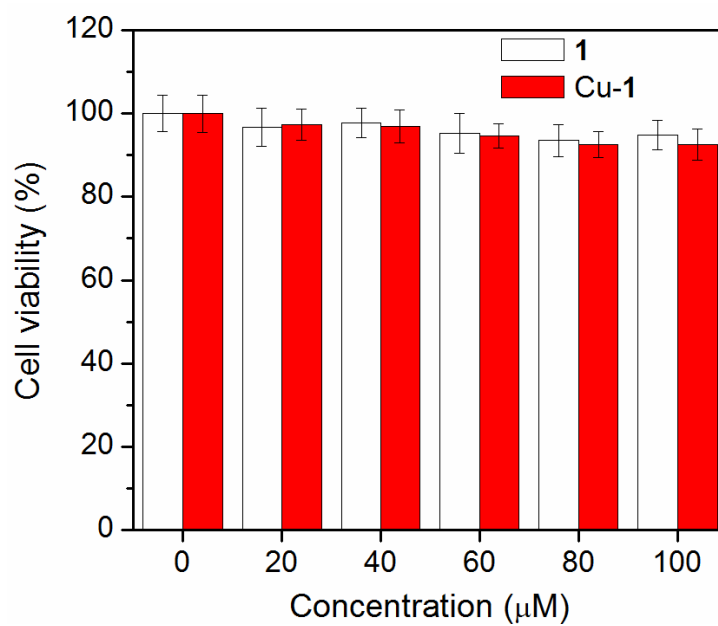


**Figure S16.** MTT assay of **1** and **Cu-1**.

### III. References

- S1 J. Olmsted, *the Journal of Physical Chemistry*, 1979, **83**, 2581.
- S2 Gaussian 09, Revision A.02, M. J. Frisch, G. W. Trucks, H. B. Schlegel, G. E. Scuseria, M. A. Robb, J. R. Cheeseman, G. Scalmani, V. Barone, B. Mennucci, G. A. Petersson, H. Nakatsuji, M. Caricato, X. Li, H. P. Hratchian, A. F. Izmaylov, J. Bloino, G. Zheng, J. L. Sonnenberg, M. Hada, M. Ehara, K. Toyota, R. Fukuda, J. Hasegawa, M. Ishida, T. Nakajima, Y. Honda, O. Kitao, H. Nakai, T. Vreven, J. A. Montgomery, Jr., J. E. Peralta, F. Ogliaro, M. Bearpark, J. J. Heyd, E. Brothers, K. N. Kudin, V. N. Staroverov, R. Kobayashi, J. Normand, K. Raghavachari, A. Rendell, J. C. Burant, S. S. Iyengar, J. Tomasi, M. Cossi, N. Rega, J. M. Millam, M. Klene, J. E. Knox, J. B. Cross, V. Bakken, C. Adamo, J. Jaramillo, R. Gomperts, R. E. Stratmann, O. Yazyev, A. J. Austin, R. Cammi, C. Pomelli, J. W. Ochterski, R. L. Martin, K. Morokuma, V. G. Zakrzewski, G. A. Voth, P. Salvador, J. J. Dannenberg, S. Dapprich, A. D. Daniels, Ö. Farkas, J. B. Foresman, J. V. Ortiz, J. Cioslowski, D. J. Fox, Gaussian, Inc., *Wallingford CT*, **2009**.
- S3 A. B. Descalzo, H. -J. Xu, Z. -L. Xue, K. Hoffmann, Z. Shen, M. G. Weller, X. -Z. You, K. Rurack, *Org. Lett.*, 2008, **8**, 1581.